Spurious Free SAW Resonators on $LiNbO_3/SiO_2$/ Quartz Substrate for Wideband Application

Yang Chen[1,2,#], Jinbo Wu[1,2,3,#] , Xiaomeng Zhao[1], Xinjian Ke[1,2], Shibin Zhang[1], Pengcheng Zheng[1,2], Kai Huang[1,*], Xin Ou[1,2,*]

[1] National Key Laboratory of Materials for Integrated Circuits, Shanghai Institute of Microsystem and Information Technology, Chinese Academy of Sciences, 865 Changning Road, Shanghai 200050 China

[2]The Center of Materials Science and Optoelectronics Engineering, University of Chinese Academy of Sciences, Beijing, 100049, China

[3]School of Information Science and Technology (SIST), ShanghaiTech University, Shanghai 201210, People's Republic of China

*Email: khuang@mail.sim.ac.cn, ouxin@mail.sim.ac.cn

[#]These authors contributed equally

***Summary*—In this work, the $LiNbO_3/SiO_2$/Quartz substrate ($LiNbO_3$-on-quartz, LNOQ) was fabricated in wafer scale using ion-cut process. 3D finite element analysis was used to design this structure. The 36°YX quartz was chosen to achieve good confinement of acoustic energy. The 42°YX LN was chosen to get large electromechanical coupling coefficient (k^2) and suppress the Rayleigh mode. The 4-inch LNOQ wafer shows high film thickness uniformity of 597.8 nm ±1.8%. The fabricated shear horizontal surface acoustic wave (SH-SAW) resonator shows large k^2 of 28.1% and high-quality factor of 959, thanks to the good confinement of acoustic energy and low RF loss of quartz. Besides, the resonators show clean out of band response due to the moderate acoustic velocity of quartz.**

***Keywords*—Surface acoustic wave resonator; $LiNbO_3$-on-quartz; spurious modes.**

I. Introduction

With the development of wireless communication technology, the filters in fifth generation (5G) era should have the characteristics such as broadband, low insertion loss and steep skirts. To realize these characteristics, the acoustic resonators, which are the key component of the acoustic filters, should have large electromechanical coupling coefficient (k^2) and high-quality factor (Q). However, the traditional surface acoustic wave (SAW) resonators fabricated using the bulk lithium niobate (LN) cannot meet these requirements due to the limited intrinsic material properties.

To promote the performance of the SAW resonators, the piezo film on hetero substrates has been proposed in recent years [1-4]. The $LiNbO_3$ (LN) who has high k^2 combined with the hetero substrates may be one of the promising choices for the high-performance broadband SAW resonators [5-7]. For the high-velocity hetero substrates, such as Si, SiC and sapphire, though they can confine the shear horizontal surface acoustic wave (SH-SAW) better, there may be high velocity spurious modes appearing at the high frequency domain owning to the high phase velocity of the substrates [5, 7-12]. These high frequency spurious modes as well as other spurious modes should be suppressed for the high-performance filters [13, 14]. For the quartz substrate, due to its moderate acoustic velocity (~5000 m/s), the high velocity spurious modes whose phase velocity is higher than 5000 m/s cannot be efficiently excited so that the resonators based on LN on quartz (LNOQ) substrate might get spurious free resonators[4, 15-17].

In this work, the 42°YX LN/SiO_2/36°YX quartz substrate was designed and fabricated. The 36°YX quartz was chosen to get good acoustic energy confinement. The SH-SAW was chosen as the main mode and the 42°YX LN was chosen to achieve high k^2 and inhibit the Rayleigh mode. This structure was fabricated in wafer scale using ion-cut process. The LN film has no void or other defect and shows excellent film uniformity of 597.8 nm ± 1.8%. The resonator based on this structure shows a large k^2 of 28.1% and maximum Bode-Q (Q_{max}) of 959. Besides, the resonator also shows clean out of band response. This structure may provide a new choice for the mass production of the broadband filters.

II. Structure Design

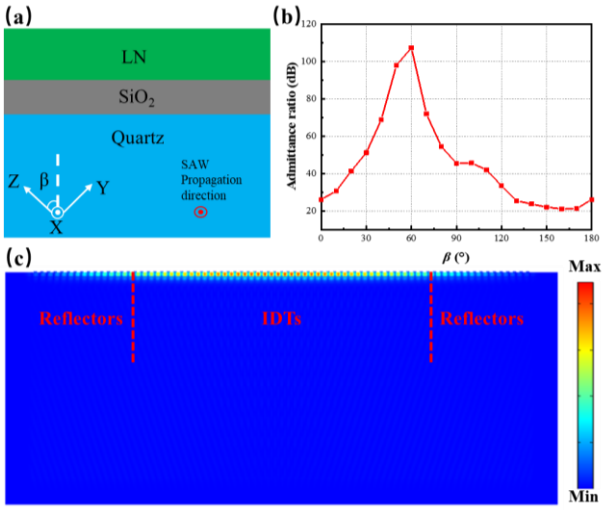

Fig. 1. (a) The schematic of the fabricated structure; (b) The simulated admittance ratio of the SAW resonators with different cut angle of quartz substrate; (c) The simulated SH-SAW resonator based on the 42°YX LN/SiO_2/36°YX quartz structure.

The structure fabricated in this paper is shown in Fig. 1(a). A SiO_2 layer is inserted between the LN film and the quartz

substrate. The rotated YX cut LN and rotated YX cut quartz are chosen to fabricate this substrate. As the quartz has high anisotropic, the rotated angle of quartz has been optimized to achieve good confinement of the acoustic energy using the 3D-finite element analysis (FEA). The LN thickness, SiO_2 thickness and the Al electrodes thickness were set as 600 nm, 200 nm and 120 nm, respectively in the simulation. The wavelength of the SAW resonator was set as 2 μm. Fig. 1(b) shows the simulated admittance ratio of the SH-SAW resonators with different rotated angle of quartz substrate. The admittance ratio gets the maximum value when β is around 60°. So, as an example, β = 54° was chosen for the quartz substrate, which corresponded to the 36°YX quartz, due to its good confinement of the SH-SAW energy in the LN film [18]. Fig. 1(c) shows the simulated SH-SAW resonator based on 42°YX LN/SiO_2/36°YX quartz structure using 2.5D FEA model and it shows good confinement of acoustic energy in the substrate surface.

To get the appropriate LN cut angle which can achieve high k^2 and clean out of band response, the SAW resonators with different rotated angle of LN are simulated using the 3D-FEA. Fig. 2(a) shows the k^2 of the Rayleigh-SAW and the SH-SAW at different cut angle of the rotated YX cut LN. The k^2 of the SH-SAW gets maximum value around 70°. However, to avoid the Rayleigh-SAW and get a clean SH-SAW response, the k^2 of the Rayleigh-SAW should be near zero. This can be achieved when the cut angle is in the range of 40-50° shown in the red region of the Fig. 2(a). As an example, the LN cut angle of 48° was chosen, which corresponds to the 42°YX LN to do the following study. Fig. 2(b) is the phase velocity of the Rayleigh-SAW and the SH-SAW varied with the cut angle of LN. The phase velocity of the Rayleigh-SAW is always smaller than the phase velocity of the SH-SAW.

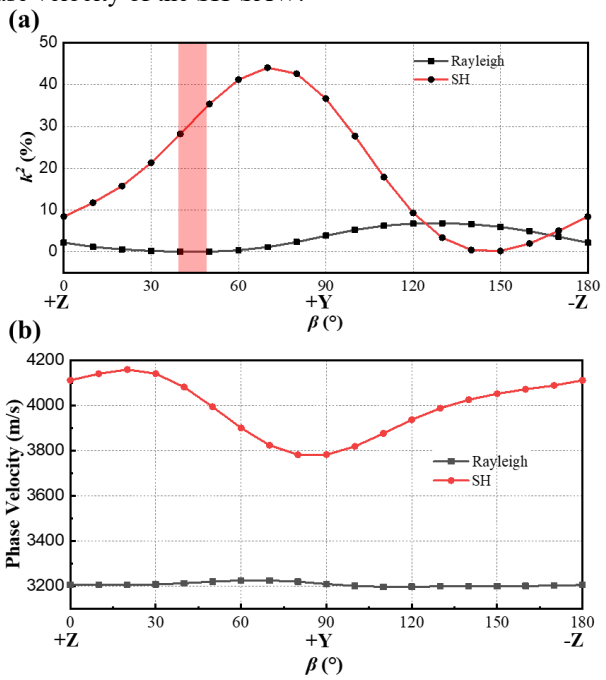

Fig. 2. (a) The k^2 of SH-SAW and Rayleigh-SAW based on the LNOQ structure at different cut angle of LN film; (b) The phase velocity of SH-SAW and Rayleigh-SAW based on the LNOQ structure at different cut angle of LN film.

The thickness of the SiO_2 interlayer also has effect on the response of the SAW resonators. Fig. 3(a) is the simulated admittance curves of the LNOQ resonators with different SiO_2 thicknesses. When the thickness of SiO_2 is larger than 300 nm, the high-order mode may be appeared around 2500 MHz. When the SiO_2 thickness is 100 nm, the Rayleigh mode around 1600 MHz might be enhanced. So, the 200 nm SiO_2 was chosen.

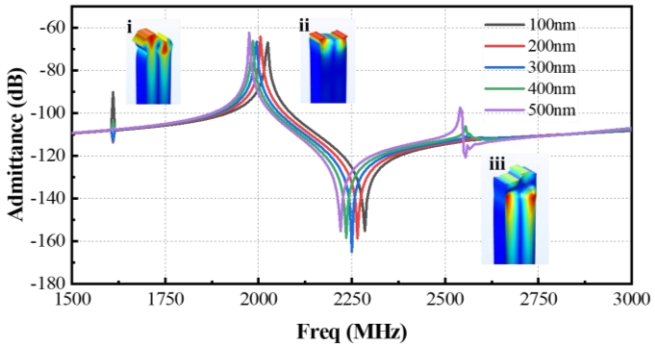

Fig. 3. The simulated admittance curves of the LNOQ SAW with different SiO_2 thicknesses.

III. Results

The LNOQ structure was fabricated based on the ion-cut process that had been demonstrated in our previous study[19]. Fig. 4(a) shows the photograph of the 4-inch wafer scale LNOQ structure. There is no void or other defect on the LN film. This is contributed to the high bonding quality of LN and quartz. Fig. 4(b) is the film thickness mapping image of the LN film measured by the white light interferometry. The LN film thickness shows high film nonuniformity (NU) of 597.8 nm ± 1.8%, which is calculated by NU = (T_{max} - T_{min})/(T_{mean}) ×100. The T_{max}, T_{min} and T_{mean} represent the maximum thickness, minimum thickness, and the average thickness of the measured LN film thickness, respectively. This low film thickness nonuniformity will facilitate the mass production of the SAW devices.

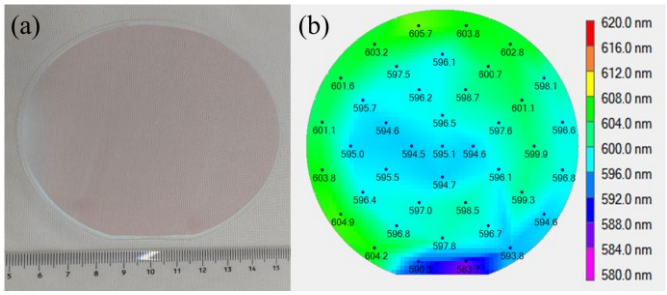

Fig. 4. (a) The image of the 4-inch wafer scale LNOQ; (b) The film thickness mapping of the LN film.

The single-port SAW resonators based on the designed LNOQ structure were fabricated and measured. The SAW resonators were fabricated based on the lift-off process. Firstly, the device patterns were formed by electron beam lithography. Then, 120 nm aluminum was deposited through electron beam evaporation and the interdigital (IDT) electrodes were then formed on the substrate through lift-off process. Different wavelengths SAW resonators were fabricated and the aperture width is 20 λ. 90.5 pairs of IDT electrodes and 50 reflection

gratings at each side were formed. Then the performance of the SAW resonator was measured by the vector network analyzer.

The admittance curves of the fabricated SAW resonators with different wavelengths are shown in Fig. 5(a). All resonators shows no Rayleigh-SAW and the high velocity spurious modes have been suppressed in almost all resonators. The resonant frequency and anti-resonant frequency increase with the wavelength and the maximum anti-resonant frequency can exceed 4 GHz. Fig. 5(b) shows the extracted k^2 of the fabricated resonators with different wavelengths. The k^2 increases with the wavelength and the maximum k^2 is 29.5 %. This indicates that the LNOQ structure has high quality.

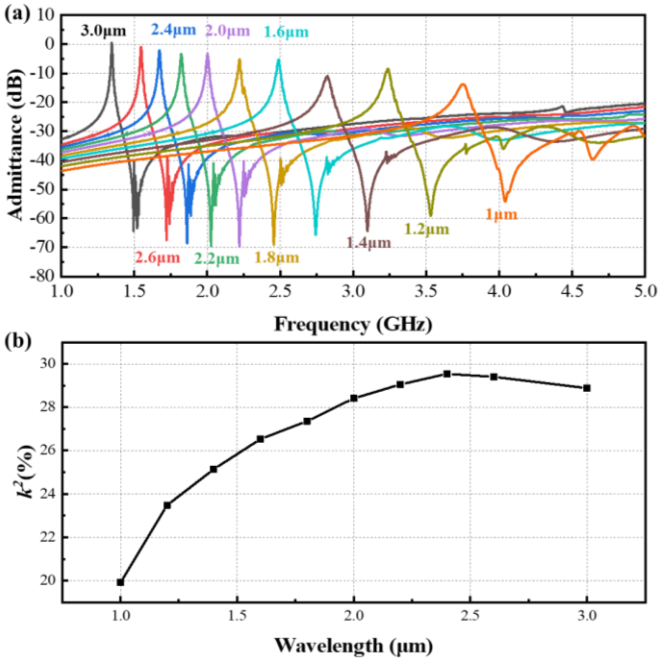

Fig. 5. (a) The measured admittance curves and conductance curves of the SAW resonators based on the LNOQ structure with different wavelength; (b) the extracted k^2 of the different wavelength SAW resonators.

When the resonators are used to fabricated SAW filters, the transverse spurious modes between the resonant frequency and anti-resonant frequency should be suppressed. Fig. 6(a) shows the measured admittance curve and conductance curve of the conventional SH-SAW resonator with 2.2 μm wavelength and its k^2 is 28.5 %. There are many transverse modes between the resonant frequency and the anti-resonant frequency. As shown on the previous research, the transverse modes can be suppressed using the tilted IDT electrodes [20]. In this paper, the IDT electrodes are tilted by 15° to realize this purpose. The optical-microscope images of the SAW resonator with tilted IDT electrodes are shown in Fig. 6. Fig. 7(c) shows the measured admittance curve and conductance curve of the SAW resonator with the tilted IDT electrodes and the extracted k^2 is 28.1%. Besides, from the conductance curve, there are no transverse modes anymore between the resonant frequency and anti-resonant frequency. It verifies the effectiveness of the tilted IDT electrodes. Fig. 7(b) and Fig. 7(d) are the Bode-Q curve of the conventional SAW resonator and the SAW resonator with tilted IDT electrodes, respectively. The SAW resonator with tilted IDT electrodes shows a higher Q value than the conventional SAW resonator with a maximum Bode-Q (Q_{max}) of 959. It means this method will not sacrifice the Q value of the resonators.

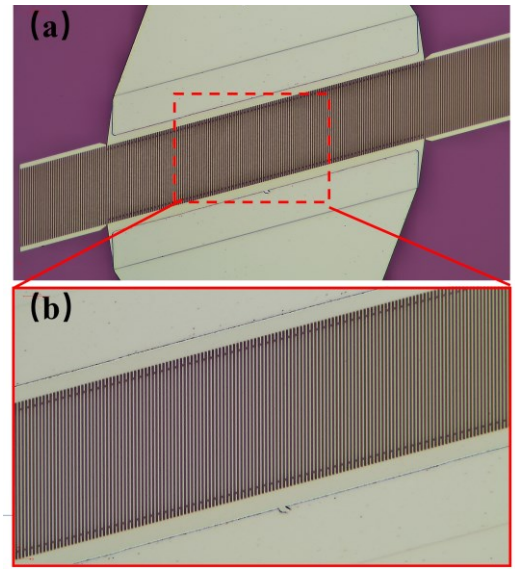

Fig. 6. The optical microscope images of the tilted SAW resonator based on the LNOQ substrate.

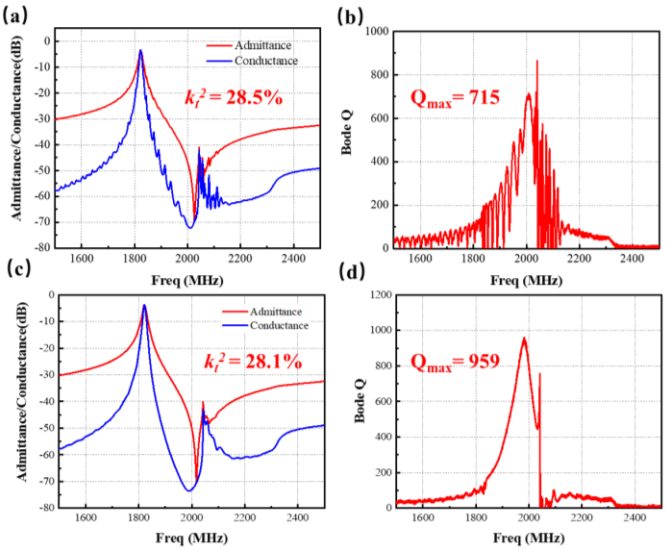

Fig. 7. (a) The measured admittance curve and conductance curve of the conventional SAW resonator based on the LNOQ structure; (b) the extracted Bode-Q curve of the conventional SAW resonator; (c) The measured admittance curve and conductance curve of the SAW resonator with tilted IDT electrodes based on the LNOQ structure; (d) the extracted Bode-Q curve of the SAW resonator with tilted IDT electrodes.

Fig. 8 shows the admittance curve and conductance curve of the SAW resonator with tilted IDT electrodes in the frequency range of 1-5 GHz. At the low frequency domain, the Rayleigh-SAW is suppressed thanks to the YX42° LN is chosen. At the high frequency domain, the high velocity modes such as longitudinal leaky surface acoustic wave (LLSAW) mode are suppressed thanks to the quartz substrate is chosen. Besides, the transverse modes between the resonant frequency and anti-frequency have been suppressed thanks to the tilted IDT electrodes is used.

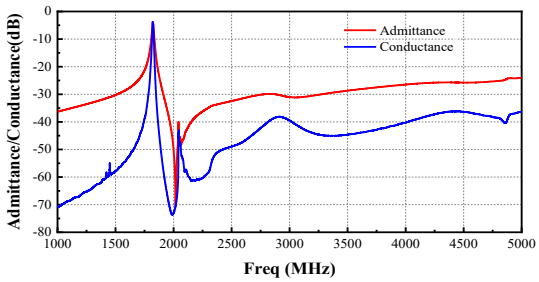

Fig. 8. The measured admittance and conductance curve of the LNOQ SAW resonator in 1-5GHz.

The last spurious mode that should be suppressed is the longitudinal spurious mode near the anti-resonant frequency of the SAW resonators. It might be suppressed through optimized the electrodes thickness in the next research. The simulated admittance curves of the SAW resonator with different Al electrode thickness are shown in Fig. 9. It shows that with the Al electrode thickness increasing, the longitudinal spurious mode gradually decays. When the thickness is 240 nm, the spurious mode can disappear.

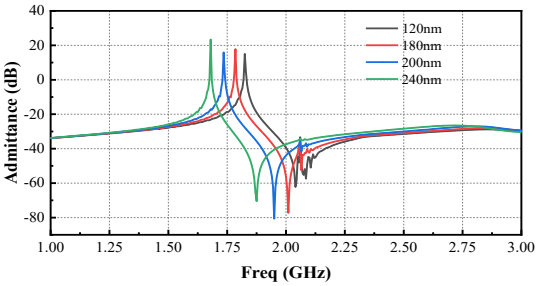

Fig. 9. The simulated admittance curves of the LNOQ SAW resonator with different electrode thickness.

IV. Conclusions

In this work, the 42°YX LN/SiO_2/36°YX quartz substrate was designed and fabricated. The 42°YX LN is chosen to inhibit the Rayleigh-SAW and get large k^2 simultaneously. The 36°YX quartz is chosen as the substrate to achieve good confinement of the SH-SAW acoustic energy and suppress the high velocity acoustic modes. The fabricated 4-inch LNOQ wafer shows low defects density and have high film uniformity of 597.8 nm ±1.8%. The resonator based on the LNOQ structure has high k^2 of 28.1% and high Q value of 959. By using the tilted IDT, the transverse modes are suppressed and the resonator shows a clean response at a wide frequency range.

Acknowledgements

This work was supported by the National key R&D Program of China (2020YFB2008801).

References

[1] T. Takai, H. Iwamoto, Y. Takamine, T. Fuyutsume, T. Nakao, M. Hiramoto, T. Toi, and M. Koshino, "High-Performance SAW Resonator With Simplified $LiTaO_3$/SiO_2 Double Layer Structure on Si Substrate," *IEEE Trans. Ultrason. Ferroelectr. Freq. Control*., vol. 66, no. 5, pp. 1006-1013, May 2019.

[2] E. Butaud, S. Ballandras, M. Bousquet, A. Drouin, B. Tavel, I. Huyet, A. Clairet, I. Bertrand, A. Ghorbel, and A. Reinhardt, "Innovative Smart Cut™ Piezo On Insulator (POI) Substrates for 5G acoustic filters," in *IEEE International Electron Devices Meeting*, 2020, pp. 34.6.1-34.6.4.

[3] S. Kakio, "High-performance surface acoustic wave devices using composite substrate structures," *Jpn. J. Appl. Phys*., vol. 6 ,no. SD0802, Jul 1 2021.

[4] S. Inoue and M. Solal, "Spurious Free SAW Resonators on Layered Substrate with Ultra-High Q, High Coupling and Small TCF," in *IEEE Ultrason. Symp*., Kobe, JAPAN, 2018 Oct 22-25 2018.

[5] S. B. Zhang, R. C. Lu, H. Y. Zhou, S. Link, Y. S. Yang, Z. X. Li, K. Huang, X. Ou, and S. B. Gong, "Surface Acoustic Wave Devices Using Lithium Niobate on Silicon Carbide," *IEEE T. Microw. Theory*., vol. 68, no. 9, pp. 3653-3666, Sept 2020.

[6] S. Wu, Z. Wu, H. Qian, F. Bao, G. Tang, F. Xu, and J. Zou, "High-performance SH-SAW resonator using optimized 30° YX-$LiNbO_3$/SiO_2/Si," *Appl. Phys. Lett*., vol. 120, no. 242201, 2022.

[7] R. Su, S. Fu, Z. Lu, J. Shen, H. Xu, Z. Xu, R. Wang, C. Song, F. Zeng, W. Wang, and F. Pan, "Over GHz bandwidth SAW filter based on 32° Y-X LN/SiO_2/poly-Si/Si heterostructure with multilayer electrode modulation," *Appl. Phys. Lett*., vol. 120, no. 253501, 2022.

[8] H. Zhou, S. Zhang, J. Wu, P. Zheng, L. Zhang, H. Xu, Z. An, T. You, and X. Ou, "Ultrawide-Band SAW Devices Using SH0 Mode Wave with Increased Velocity for 5G Front-Ends," in *IEEE Ultrason. Symp*., 2021, pp. 1-4.

[9] P. C. Zheng, S. B. Zhang, H. Y. Zhou, L. P. Zhang, J. B. Wu, H. L. Yao, K. Huang, X. M. Zhao, T. G. You, and X. Ou, "Ultra-Low Loss and High Phase Velocity Acoustic Delay Lines in Lithium Niobate on Silicon Carbide Platform," in *IEEE Micro. Electro. Mech. Syst*., 2022, pp. 1030-1033.

[10] J. Wu, S. Zhang, H. Zhou, L. Zhang, P. Zheng, Z. Li, Y. Wang, K. Huang, T. You, T. Wu, and X. Ou, "Low-Loss SAW Devices with $LiTaO_3$ on Extremely High Resistance Substrate," in *IEEE Ultrason. Symp*., 2021, pp. 1-4.

[11] J. Shen, S. Fu, R. Su, H. Xu, Z. Lu, Z. Xu, J. Luo, F. Zeng, C. Song, W. Wang, and F. Pan, "High-Performance Surface Acoustic Wave Devices Using $LiNbO_3$/SiO_2/SiC Multilayered Substrates," *IEEE T. Microw. Theory.*, vol. 69, no. 8, pp. 3693-3705, 2021.

[12] M. Gomi, T. Kataoka, J. Hayashi, and S. Kakio, "High-coupling leaky surface acoustic waves on $LiNbO_3$ or $LiTaO_3$ thin plate bonded to high-velocity substrate," *Jpn. J. Appl. Phys.*, vol. 56, no. 07JD13, Jul 2017.

[13] R. Goto, H. Nakamura, and K. Hashimoto, "The modeling of the transverse mode in TC-SAW using SiO_2/$LiNbO_3$ structure," *Jpn. J. Appl. Phys.*, vol. 58, no. SGGC07, Jul 1 2019.

[14] Y. W. He, Y. P. Wong, Q. Liang, T. Wu, J. F. Bao, and K. Y. Hashimoto, "Double Busbar Structure for Transverse Energy Leakage and Resonance Suppression in Surface Acoustic Wave Resonators Using 42 degrees YX-Lithium Tantalate Thin Plate," *IEEE Trans. Ultrason. Ferroelect. Freq. Contr.*, vol. 69, no. 3, pp. 1112-1119, Mar 2022.

[15] N. F. Naumenko, "Temperature Behavior of SAW Resonators Based on $LiNbO_3$/Quartz and $LiTaO_3$/Quartz Substrates," *IEEE Trans. Ultrason. Ferroelectr. Freq. Control.*, vol. 68, no. 11, pp. 3430-3437, Nov 2021.

[16] M. Kadota and S. Tanaka, "Improved Quality Factor of Hetero Acoustic Layer (HAL) SAW Resonator Combining $LiTaO_3$ Thin Plate and Quartz Substrate," in *IEEE Ultrason. Symp.*, 2017,

[17] S. Inoue and M. Solal, "LT/Quartz Layered SAW Substrate with Suppressed Transverse Mode Generation," in I*EEE Ultrason. Symp*., Las Vegas, NV, 2020 Sep 07-11 2020, in *IEEE International Ultrasonics Symposium*, 2020,

[18] Y. Chen, J. Wu, X. Zhao, Z. Li, X. Ke, S. Zhang, M. Zhou, K. Huang, and X. Ou, "Heterogeneous integration of lithium tantalate thin film on quartz for high performance surface acoustic wave resonator," *Jpn. J. Appl. Phys.*, vol. 62, no. 015503, 2022.

[19] Y. Chen, J. B. Wu, X. M. Zhao, Z. X. Li, X. J. Ke, S. B. Zhang, M. Zhou, K. Huang, and X. Ou, "Heterogeneous integration of lithium tantalate thin film on quartz for high performance surface acoustic wave resonator," *Jpn. J. Appl. Phys.*, vol. 62, no. 1, Jan 1 2023.

[20] H. Iwamoto, T. Takai, Y. Takamine, T. Nakao, T. Fuyutsume, and M. Koshino, "Transverse Modes in IHP SAW Resonator and Their Suppression Method," 2018 *IEEE International Ultrasonics Symposium (IUS)*, 2018.